The Bolivian Altiplano conductivity anomaly

Heinrich Brasse,[1] Pamela Lezaeta,[1,2] Volker Rath,[1,3] Katrin Schwalenberg,[4,5] Wolfgang Soyer,[1] and Volker Haak[4]

Received 28 March 2000; revised 25 October 2001; accepted 14 November 2001; published 22 May 2002.

[1] A long-period magnetotelluric study was carried out in the central Andes between latitudes 19.5°S and 21°S along two almost parallel profiles of 220 and 380 km length, respectively. The investigation area extends from the Pacific coast to the southern Altiplano Plateau in the back arc of the South American subduction zone. The main geoelectrical structure resolved is a broad and probably deep-reaching highly conductive zone in the middle and deeper crust beneath the high plateau. Although the data show deviations from two-dimensionality, a two-dimensional approach is justified for large parts of the profiles. Sensitivity studies were carried out in order to constrain the depth extent. Another electrically conductive structure was resolved in the middle crust of the Chilean forearc, thought to be connected with the Precordillera fault system. The Andean Continental Research Program (ANCORP) seismic reflection profile, carried out along the same line at 21°S, revealed highly reflective zones below the Altiplano, in good correlation with the upper boundary of the Altiplano conductor. This highly conductive domain also coincides with low seismic velocities and a zone of an elevated v_p/v_s ratio and, although not well resolved, with low Q_p seismic quality factors. Taking into account the enhanced heat flow and a derived temperature model, the most probable explanation lies in the assumption of granitic partial melts. The good conductor below the volcanic arc which was found in regions farther south at 22°S gradually vanishes toward the north; this is consistent with the results of seismic tomography concerning Q_p values and a gap of recent volcanism. *INDEX TERMS:* 1515 Geomagnetism and Paleomagnetism: Geomagnetic induction; 8124 Tectonophysics: Earth's interior—composition and state; 5109 Physical Properties of Rocks: Magnetic and electrical properties; 9360 Information Related to Geographic Region: South America; *KEYWORDS:* magnetotellurics, 2-D inversion, partial melts, Andes, Bolivia, Chile

1. Introduction and Geological Setting

[2] In the convergence zone of the oceanic Nazca Plate and the continental South American Plate the central Andes of southern Peru, southwestern Bolivia, northern Chile, and northwestern Argentina form the great Altiplano-Puna high plateau. Bounded by the Eastern Cordillera to the east and the Precordillera in the west, it reaches mean altitudes of ~3700 m in the Bolivian Altiplano and ~4500 m in the Chilean-Argentinian Puna. Between the Precordillera and the Altiplano proper lies the volcanic arc of the Western Cordillera with active volcanoes reaching elevations of over 6000 m (Figure 1). Crustal thickness is estimated at 70 km below the Altiplano [*James*, 1971; *Wigger et al.*, 1994; *Götze et al.*, 1994; *Beck et al.*, 1996, 1999]. The cause of the thickened crust below the plateau and the uplift of the plateau as an isostatic response to crustal thickening (magmatic underplating, crustal shortening, or a combination of both) is still controversial [see, e.g., *Isacks*, 1988; *Schmitz*, 1994; *Allmendinger et al.*, 1997; *Lamb and Hoke*, 1997; *Okaya et al.*, 1997; *Giese et al.*, 1999].

[3] The volcanoes of the Western Cordillera form part of the Central Volcanic Zone (CVZ) of the Andes. The CVZ is confined to the region of relatively steep subduction of the Nazca Plate with a subduction angle of 30° at a depth of 100 km [*Isacks*, 1988]. The position of the volcanic arc has experienced an eastward shift since the Jurassic from what is today the Coastal Cordillera to the actual Western Cordillera [*Scheuber*, 1994]. North of 16°S and south of 28°S, active volcanism vanishes, correlating with a shallower subduction. In the investigation area of this study between 19.5°S and 21°S, however, a gap of recent volcanism exists north of 21°S, the so-called Pica gap, named after the Altos de Pica, an area in the Precordillera characterized by a large cover of ignimbrites [*Wörner et al.*, 1994].

[4] Several large shear zones traverse the studied segment of the central Andes: the Atacama Fault System (AF) in the Coastal Cordillera, the Falla Oeste or West Fissure (WF) in the Precordillera, and the Uyuni-Kenyani Fault running transversely from the eastern Altiplano to the Western Cordillera in Chile. The AF and WF run mainly N-S and are thought to be due to the slightly oblique convergence of the Nazca Plate (and the earlier Farallon and Aluk) and South American Plate, respectively. The direction of strike-slip movement of these predominant fault zones changed from sinistral to dextral and vice versa [*Scheuber*, 1994]. Along the West Fissure are encountered some of the largest porphyry copper deposits in the world, e.g., Chuquicamata or, more closely related to the investigation area, the mines of Quebrada Blanca and Collahuasi.

[5] The Chilean part of the study area comprises one of the most arid regions of the world: the Atacama desert. Several large salt flats, i.e., the Salar Grande in the Coastal Cordillera and the Salar de Uyuni on the Altiplano, are further characteristics of the measuring area which severely impede magnetotelluric work due

[1]Fachrichtung Geophysik, Freie Universität Berlin, Berlin, Germany.
[2]Now at Woods Hole Oceanographic Institution, Woods Hole, Massachusetts, USA.
[3]Now at Rheinisch-Westfälische Technische Hochschule, Aachen, Germany.
[4]GeoForschungsZentrum, Potsdam, Germany.
[5]Now at Department of Physics, University of Toronto, Toronto, Ontario, Canada.

0148-0227/02/2001JB000391$09.00

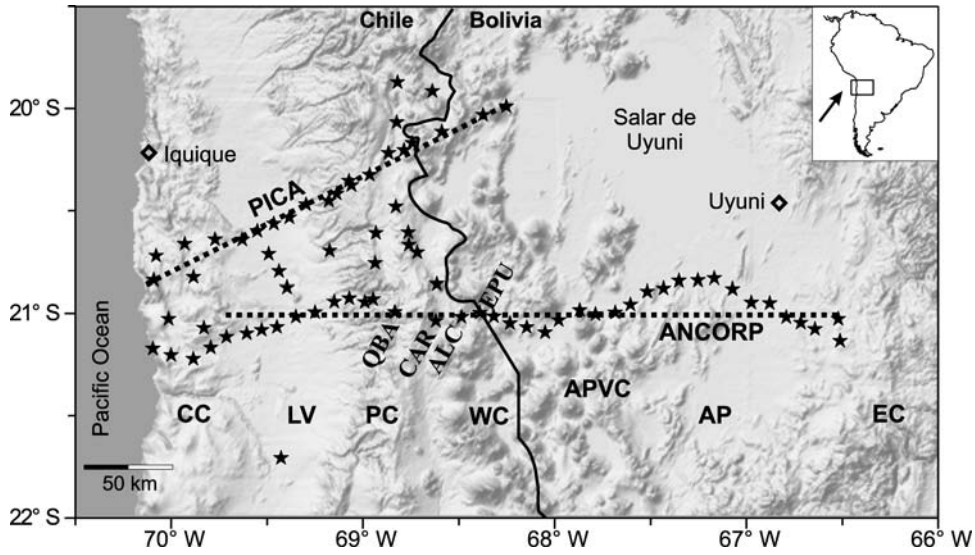

Figure 1. Shaded relief map of the investigation area in northern Chile and southwestern Bolivia. Stars indicate measured magnetotelluric (MT) sites. CC, Coastal Cordillera; LV, Longitudinal Valley; PC, Precordillera; WC, Western Cordillera; APVC, Altiplano-Puna Volcanic Complex; AP, Altiplano; EC, Eastern Cordillera. The ANCORP profile extends over 380 km from the Pacific coast to the margin of the Eastern Cordillera, while the PICA profile covers a length of 220 km from the coast to the edge of the Salar de Uyuni, a vast salt plain unsuitable for MT measurements. Dotted lines indicate data sets which were used for 2-D modeling.

to inaccessibility and often problematically high contact resistances of electrodes. The Peru-Chile oceanic trench, being almost free of sediments [*von Huene et al.*, 1999] due to long-time aridity of the western central Andes, is 7–8 km deep; the ocean conductance thus exceeds 20,000 S, and an extremely strong coast effect has to be expected which may blur other anomalies near the coast.

[6] During the last years, several large electrical conductivity anomalies were detected beneath the southern central Andes in northern Chile, SW Bolivia, and NW Argentina [e.g., *Schwarz and Krüger*, 1997; *Echternacht et al.*, 1997; *Lezaeta et al.*, 2000]. While *Schwarz and Krüger* [1997] report an extensive zone of enhanced electrical conductivity below the volcanic arc at 22°S latitude, *Echternacht et al.* [1997] modeled a good electrical conductor below the Precordillera and related this anomaly to the West Fissure. The anomaly below the volcanic arc was interpreted as a vast zone of partial melts in the middle and lower crust [see also *Schilling et al.*, 1997], whereas the Precordillera anomaly was explained by rising saline fluids from the deeper crust or even the downgoing slab.

[7] The present study, carried out within the framework of the Collaborative Research Programme SFB 267 Deformation Processes in the Andes, is an extension of this work. A magnetotelluric profile was conducted in 1997 and 1998 along latitude 21°S traversing the Andes from the Pacific Coast to the margins of the Eastern Cordillera (Figure 1). This profile (called ANCORP from Andean Continental Research Programme) was part of a large-scale geoscientific study which also comprised a seismic reflection/refraction profile and a passive seismological experiment [*ANCORP Working Group*, 1999]. The previously mentioned magnetotelluric (MT) profile of *Echternacht et al.* [1997], which we will refer to as the PICA profile (after the oasis village of Pica in northern Chile), was extended toward the Salar de Uyuni. Additionally, intermediate sites were built up in between these profiles in the forearc to investigate for possible or already known three-dimensional structures.

[8] Altogether 14 long-period magnetotelluric (LMT) instruments were employed with fluxgate magnetometers and low-energy consumption data loggers; the period range covered 10 s to several tens of thousands of seconds. To guarantee an overlapping of adjacent sites with respect to midcrustal and lower crustal investigation depths, a site separation of ~10 km was chosen. Individual stations operated for 3–4 weeks continuously; all 14 stations were synchronized by GPS receivers. In addition, at several sites an audiomagnetotelluric (AMT) device (period range 0.001–100 s) was operated to control the transfer functions at short LMT periods and to study the conductivity distribution at shallower depths.

[9] The ANCORP profile traverses the main morphological units of the central Andes from the coast via the Coastal Cordillera, the Longitudinal Valley, the Precordillera, the Western Cordillera, and the Bolivian Altiplano. Because of the lack of passable roads, the profile could not be laid out as a straight line. The Quebrada Huatacondo, a narrow, ~30 km long E-W gorge traversing the western part of the Precordillera, is the only pathway across the Andes at this latitude. The profile crosses the West Fissure inside the gorge; here a more closely spaced AMT profile was conducted to study the near-surface conductivity distribution related to the fault. We cannot rule out topographic effects along this stretch of the main profile which might even be enhanced by better conductive sedimentary fillings inside the gorge; the AMT results, however, show "normal" surficial resistivities of a few hundred ohm meters compared with the surroundings [*Janssen et al.*, 2001]. Selection of suitable LMT sites was hindered by the recent expansion of mining activity in the Precordillera (Quebrada Blanca and Collahuasi), which led to a certain gap of measuring points between sites QBA and CAR (see Figure 1; for a complete list of site names see Figure 2). Between ALC and EPU on the Chile-Bolivia border the profile passes just south of a volcanic ridge displaying fumarolic activity and two potentially active centers, the Olca and Paruma volcanoes [*de Silva and Francis*, 1991]. The volcanic front proper begins with Pabellon del Inca volcano immediately north of site CAR. On the Bolivian side of the profile the recent volcanism of the Western Cordillera slowly vanishes and gives way to the so-called Altiplano-Puna Volcanic Complex (APVC) with several Miocene-Pliocene centers [*de Silva*, 1989]. The Bolivian Altiplano is covered by a large pile of sediments, with thicknesses deduced from industrial reflection seismology of up to 10 km in some parts. As will be shown in sections 4 and 5,

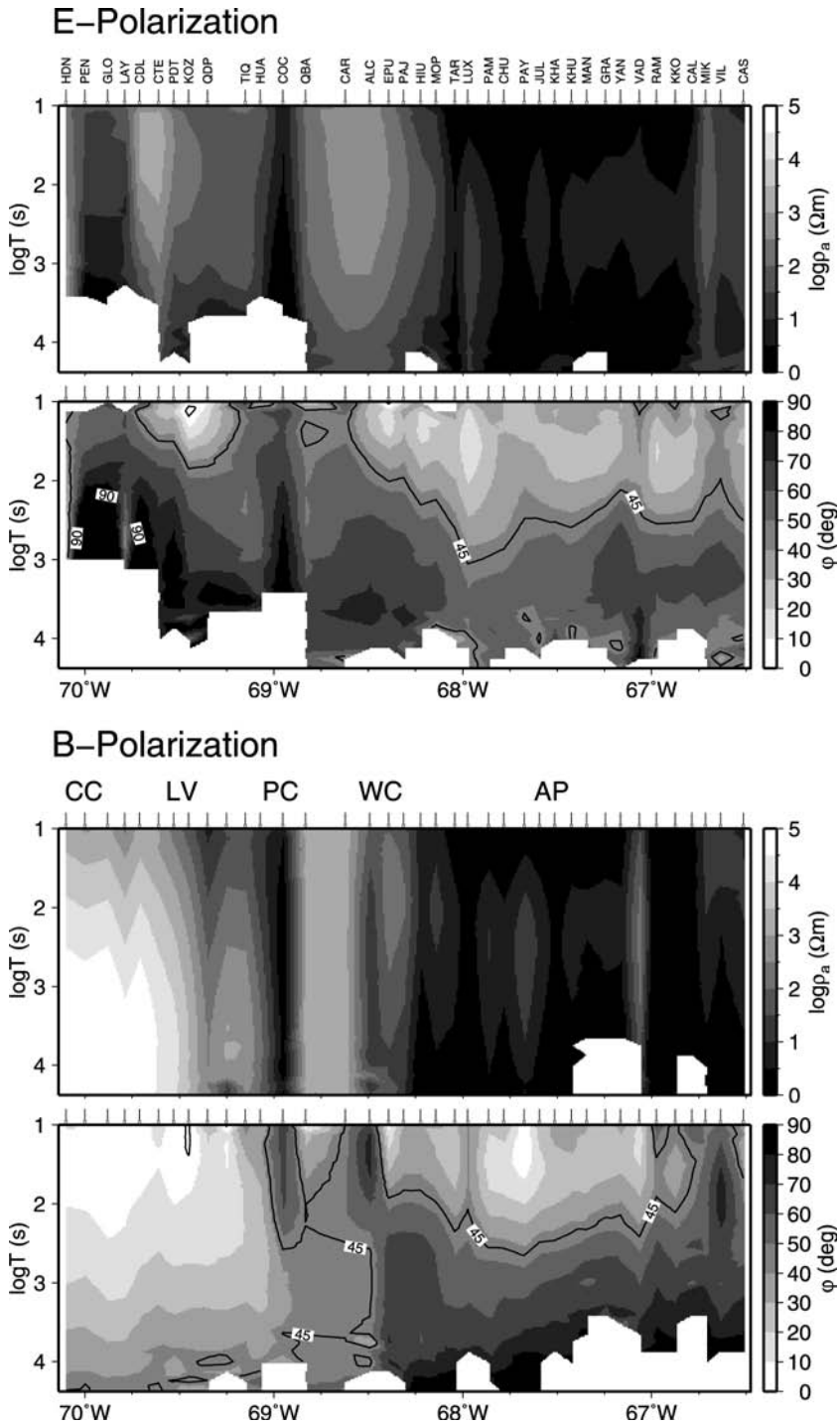

Figure 2. Pseudosections of apparent resistivities and phases for (top) the *xy* component E polarization or TE mode, and (bottom) the *yx* component (B polarization or TM mode) of the unrotated impedance tensor. Scattered and low-quality data at longer periods are blanked out.

this leads to a reduced depth of penetration of the natural electromagnetic field variations.

2. Data Processing

[10] A program package developed by *Egbert and Booker* [1986] was used to calculate the electromagnetic transfer functions. First, isolated outliers were removed in time domain using a running median filter. Also, for some of the sites, bad data segments were visually identified and excluded from further processing. Then, within a seven-level cascaded decimation scheme of decimation factor 4 data were prewhitened by an adaptive, autoregressive filter and windowed to a length of 128 samples for the Fourier transformation. Robust single-station and remote reference bivariate local transfer functions (MT impedance tensor **Z** and magnetic transfer functions T_{zx} and T_{zy}) were

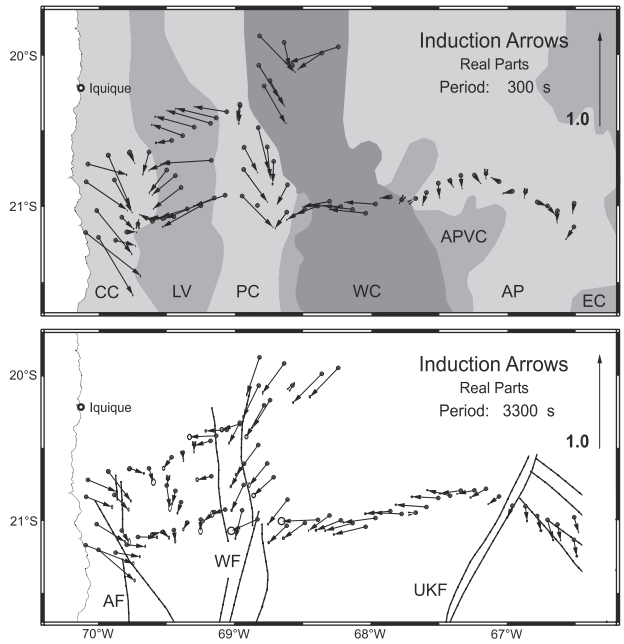

Figure 3. Real induction arrows for periods of 300 and 3300 s. Also shown are (top) the main morphological units (for abbreviations, see Figure 1) and (bottom) major tectonic faults with AF, Atacama Fault; WF, West Fissure; and UKF, Uyuni-Kenyani Fault.

calculated using the regression M estimate described by *Egbert and Booker* [1986]:

$$\begin{bmatrix} E_x \\ E_y \\ B_z \end{bmatrix} = \begin{bmatrix} Z_{xx} & Z_{xy} \\ Z_{yx} & Z_{yy} \\ T_{zx} & T_{zy} \end{bmatrix} \begin{bmatrix} B_x \\ B_y \end{bmatrix},$$

with B the magnetic field, E the electric field, and x, y referring to geomagnetic north and east, respectively. Low excitation energy led to strong downward bias in impedance magnitude due to correlated noise in the magnetic fields between 10 and 100 s and remote reference processing [*Gamble et al.*, 1979] proved to be necessary and very successful in this specific period range. It did not enhance data quality at long periods, however. The most unperturbed stations were chosen as reference, e.g., CTE in the Longitudinal Valley, which operated continuously during the whole 1998 campaign.

[11] Figure 2 displays the MT data as pseudosections of apparent resistivities $\rho_a(T)$ and phases $\varphi(T)$ calculated from the minor diagonal of the unrotated impedance tensor; that is, data for all sites are plotted as function of period T in a geomagnetically N-S/E-W oriented coordinate system. In the study area the magnetic declination is only 1–2° as was calculated from the International Geomagnetic Reference Field 1995 (IGRF95) data; thus geomagnetic and geographic directions basically coincide. In anticipation of section 3 we assign the xy component to the E polarization (or TE mode for tangential electric), where the electric field is parallel to the lateral conductivity contrasts, i.e., N-S oriented, and the yx component to the B polarization (or TM mode for tangential magnetic) with the magnetic field parallel and the electric field transversal (EW) to the lateral boundaries.

[12] The most prominent features of the data can clearly be identified in Figure 2:

1. Data from the western part of the profile are dominated by the coast effect. The low apparent resistivities in the E polarization at most stations in the Coastal Cordillera are connected with very high phases close to 90° or even higher. This is at least partly due to extremely strong distortions, which will be analyzed in a future paper.

2. Beneath the western Precordillera, at short periods, a good conductor can be observed in both polarizations.

3. Unlike in areas farther south, there is no indication of a highly conducting volcanic arc, except possibly at the eastern boundary of the Western Cordillera.

4. A large high-conductivity anomaly is located beneath the Altiplano, underlying shallow, high-conductivity sediments and a moderately resistive crystalline upper crust.

5. Strong static shifts (a parallel offset of apparent resistivity curves over a broad period range until DC due to surficial small-scale lateral inhomogeneities) can be observed at several sites, e.g., at VAD on the eastern Altiplano, where the station was built on outcropping more compacted, and thus more resistive, paleozoic sediments compared to the surrounding quaternary deposits.

[13] Induction arrows, derived from the real parts of the transfer functions T_{zx} and T_{zy}, are shown in Figure 3 for two representative periods, sampling structures at intermediate and large depths. In the so-called Wiese convention they should point away from conductors in a two-dimensional setting. Though the trench is 7–8 km deep and thus represents a strong roughly N-S oriented conductivity contrast, induction arrows show a significant deviation from E-W in the Coastal Cordillera. This cannot be explained by directional changes of the trench nor by a varying coastline, so the cause must lie in strong upper crustal and midcrustal anomalies near the coast.

[14] For 300 s, in the western Longitudinal Valley the influence of the ocean to the vertical magnetic field seems already to be compensated by that of a good conductor under the Precordillera, which might be bent to the west between the two profiles. To the east of this anomaly, arrows point significantly N-S over the entire study area, which could be attributed to increasing conductances toward the north. At the eastern margin of the Western Cordillera, arrows indicate a high-conductivity contrast below the Altiplano, whereas the Altiplano itself is relatively one-dimensional (1-D) for that period.

[15] At longer periods, the influence of the Precordillera anomaly on the magnetic field decreases, and the conductivity contrast to the Altiplano becomes visible at numerous sites. In addition, the Uyuni-Kenyani Fault on the eastern Altiplano (Figure 3) seems to affect the induction arrows in a remarkably symmetric manner. To the NE of the northernmost sites on the PICA profile and thus below the central Altiplano, extraordinary high conductivities are indicated in this period range. This structure lies outside the study area, and therefore no further information can be deduced concerning its western margin and depth.

[16] Altogether and at first sight, the observed magnetic transfer functions appear more complicated than the MT impedances and indicate two-dimensionality only for parts of the investigation area. However, 3-D modeling studies of the forearc have been carried out in the meanwhile [*Lezaeta*, 2001] showing main conductive structures that are still roughly N-S oriented. Near the coast, high conductivities are associated with the Atacama Fault System (oriented N5°W–N10°W). Alternatively, the deflection of induction arrows could also be explained by modeling the Atacama Fault as an anisotropic 2-D structure [*Beike*, 2001].

[17] The above mentioned 3-D studies also show that the Precordillera is characterized by an N-S running conductive structure with increasing conductances toward the north (see also the inversion results for both profiles in section 4). Such an internal differentiation of a conductive feature is easily overseen by looking only at impedances (which are less sensitive in such a case) on a single profile, and as a consequence, the MT data appear as basically 2-D (as described in section 3) and a 2-D approach for the MT transfer functions may still be justified.

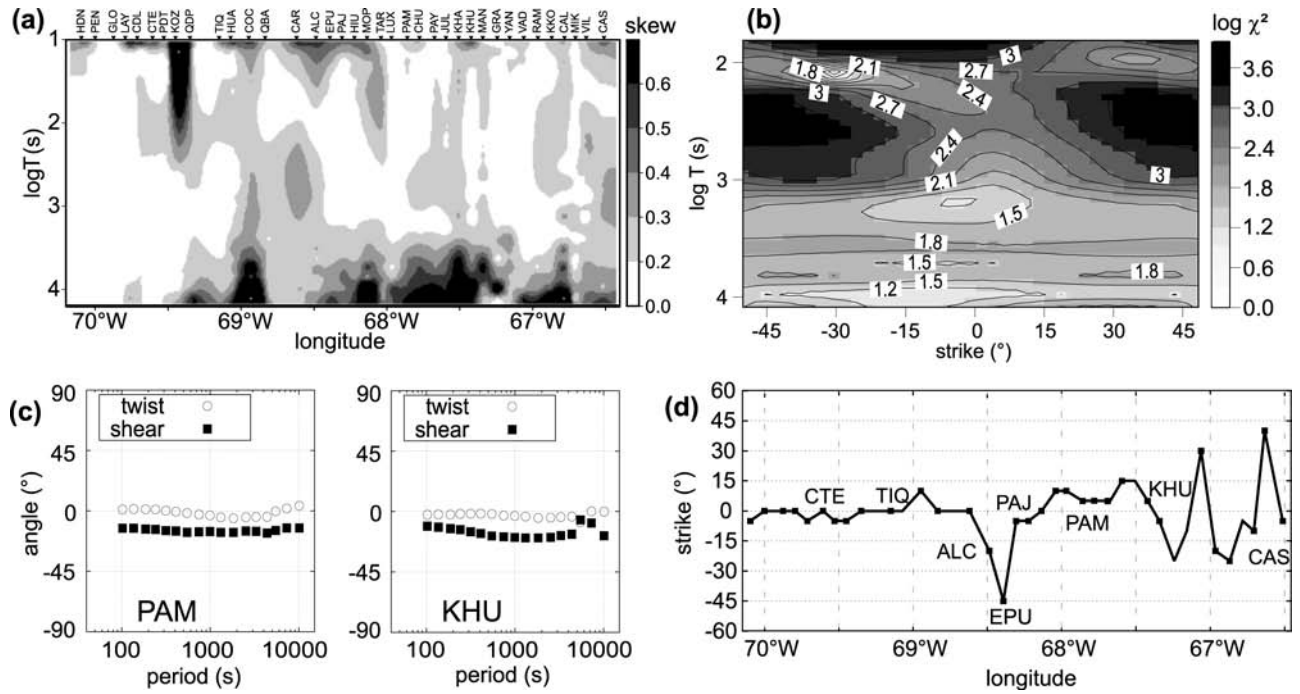

Figure 4. Procedure to find the regional strike along the ANCORP profile. (a) Contour plot of phase-sensitive regional skew [*Bahr*, 1988] along the ANCORP profile. (b) The χ^2 misfit after *Groom and Bailey* [1989] decomposition, illustrated for site PAM. (c) Twist and shear distortion parameters for a fixed strike angle of 0° at sites PAM and KHU. (d) Period-averaged regional magnetotelluric strike directions for the sites along the ANCORP profile in the period range between 1000 and 6000 s. The outliers at sites ALC and EPU, located directly below active Olca volcano in the Western Cordillera, may result from additional magnetic distortion, which was not included in the calculation of regional strikes.

[18] Owing to the strong distortions and phases above 90°, we excluded the five sites in the Coastal Cordillera (HDN to LAY) from the 2-D interpretation approach described in the following sections. For the main anomaly below the Altiplano studied here (besides the ocean) the induction arrows justify a two-dimensional approach. This will also be seen in the MT impedances in sections 4 and 5.

3. Dimensionality of MT Transfer Functions

[19] Before considering any 2-D modeling or inversion, data have to be analyzed to determine whether a consistent regional strike can be found for the whole profile or at least some parts of it. As a first step, we investigate the dimensionality of the data. On the basis of the hypothesis that telluric distortion (i.e., shallow 3-D anomalies overly a regional 2-D structure) affects the impedance tensor, we calculated the rotationally invariant phase-sensitive or regional skew parameter defined by *Bahr* [1988, 1991] as a function of period for each site. In a coordinate frame x'-y' aligned with the regional 2-D conductivity contrast (if existing) the tensor elements $Z_{x'x'}$ and $Z_{y'x'}$ (as well as $Z_{x'y'}$ and $Z_{y'y'}$) should have equal phases [*Bahr*, 1991]. The skew parameter measures the phase difference between each pair of tensor elements and thus indicates a departure from the assumption of two-dimensionality. It may also be interpreted as a measure of telluric distortion, whenever the superposition model is valid. In the case of a perfect 2-D earth it will be zero, whereas values above 0.3 can be considered as an indicator of true 3-D inductive regional structures and the validity of the superposition model must be questioned [*Bahr*, 1988].

[20] A contour plot of this skew parameter as a function of period along the ANCORP profile is shown in Figure 4a. The values are mostly small and support the assumption of a 2-D Earth at most of the sites. Greater skew values over a large period range are observed at site KOZ in the Longitudinal Valley, several sites in the Precordillera and on the eastern Altiplano (e.g., CAS).

[21] Furthermore, impedance tensors were decomposed using the well-known decomposition scheme of *Groom and Bailey* [1989], which is based on the same 2-D regional superposition model and quantifies the degree of telluric distortion. The most important parameter yielded by this method is the regional strike direction. The decomposition was calculated for each site by varying the strike angle stepwise by 5° between −45° and 45°, calculating the χ^2 misfit between measured and decomposed impedances for each fixed value. This procedure is illustrated in Figure 4b for site PAM, showing that the best fit over a wide period range can be found at the 0° strike angle, indicating a N-S orientation of the regional structure. Strike angle fixed, twist, and shear angles can be seen to be nearly independent of frequency. An example of this procedure is shown for sites PAM and KHU, located in the Altiplano (Figure 4c).

[22] For all sites along the profile a strike angle was determined by calculating an average minimum misfit in the period range between 1000 and 6000 s, which contains the relevant information about the major deep structures in the area (compare Figure 2). Figure 4d shows that the angles vary between ±10° in the western part of the profile. Some sites located in the eastern Altiplano as well as two sites (ALC, EPU) in the Western Cordillera show great deviations from this direction. Sites ALC and EPU are located directly below active Olca volcano; here the distortion is frequency-dependent which is indicative for an inductive effect. The sites in the eastern Altiplano show greater departures from the expected regional 2-D model, indicated also by larger skew values (Figure 4a). This is also consistent with the direction of the induction arrows (real parts) in this area (see Figure 3), which display a large south component.

[23] The impedance tensor and magnetic transfer functions were also analyzed with the decomposition method of *Chave and Smith* [1994], including also magnetic distortion with azimuths ranging between ±90°. The strike angles showing the smallest averaged misfit vary in a much broader range from site to site (not shown here), with the greatest departures from the N-S direction (i.e., 0°) in the data of the Coastal Cordillera, and the eastern Altiplano, with values around +60° and ±70°, respectively. Nevertheless, data from the Western Cordillera (with the exception of ALC and EPU) and the western Altiplano (sites PAJ to MAN) show angles near 0°. All these strike angles are similar to the ones deduced from induction arrow directions.

[24] For this study we assumed a regional 2-D structure striking N-S (0°), i.e., the direction of the Andean mountain belt, at least for investigation depths >20 km, although this may not be justified in detail in the problematic areas. Further investigations should clarify and explain the obvious discrepancy between the induction arrows and the strike direction obtained from MT data. Two-dimensional anisotropic and/or 3-D models may explain this, and the analysis of the full data set in the area (see Figure 1) is necessary but beyond the scope of this article.

4. A 2-D Interpretation: Inversion and Modeling Results

[25] In section 3 we determined that at least the eastern part of the profile can be treated as 2-D, though 3-D influences are clearly visible in some problematic areas (Coastal Cordillera, Precordillera, and the eastern Altiplano). In this section we will give a 2-D interpretation of the data from the ANCORP profile (dotted line at 21°S in Figure 1), leaving the five westernmost sites for future 3-D modeling.

[26] We used the 2-D inversion code of *Mackie et al.* [1997] [see also *Rodi and Mackie*, 2001] to jointly invert E and B polarization resistivities and phases. In this code the strongly ill-posed nonlinear inverse problem of calculating the subsurface conductivity distribution from magnetotelluric data is solved by the optimization of an objective function, which consists of a least squares measure of misfit between observed and modeled data and a regularizing term. This constraint is realized by simply taking differences between the logarithmic resistivities of adjacent grid elements. As a graded grid was used (which is common in broadband electromagnetic modeling), this procedure may lead to artifacts if vertical and horizontal grid spacings are very different. Therefore grid spacing was kept as uniform as possible within the region of interest.

[27] The behavior of the inversion process is controlled by two weighting factors, namely, a trade-off parameter τ reflecting the compromise between fitting the data and model smoothness and a Marquardt-type damping constant ε to stabilize the inversion process in early iterations. By systematical studies an optimal value for the former was found at $\tau = 10$, while the latter was fixed at $\varepsilon = 0.001$.

[28] For all models shown in this paper the inversion started from a homogeneous half-space of 20 Ω m, a kind of average value for the resistivities in the forearc and the back arc. Other starting models were tested, also on data subsets like the Bolivian part alone; they all yielded similar results. Although the coast line is 40 km west of the westernmost site CTE, the Pacific Ocean produces a huge coast effect which can be seen far inland, and we included it, with a coarse bathymetry, as a priori information. Further a priori models were used to test hypotheses derived from other geophysical methods and will be described later. In that case, the algorithm is forced to find a solution, which deviation from the a priori model has to be smooth [*Mackie et al.*, 1997].

[29] Decomposition leaves the problem of indeterminacy of the real factors shifting the principal apparent resistivities from their true values, with phases undistorted. We assigned minimum error floors of 20% for $\ln \rho_a$ and 1° for φ, thus downweighting the apparent resistivities with respect to the phases. As expected, this leads to smooth models with excellent data fit in φ and large deviation in $\ln \rho_a$, though the shape of the curves is reproduced correctly. In principle, this static shift can be corrected automatically during each iteration. However, numerical experiments show that in early stages of the inversion process, substantial information may erroneously be transferred to static shifts. Therefore these factors were calculated from the response of the final model in Figure 5, where the measure of misfit has already converged to a plateau, with respect to the observed data.

[30] Figure 5 (top) shows an inversion result after 30 iterations where the misfit function has converged to a constant level. In general, the model shows high resistivity values in the forearc region (>1000 Ω m) and low resistivity values in the back arc (∼1 Ω m). This can easily be verified by observing the data (Figure 2): Apparent resistivities in the west are orders of magnitude greater than those in the east. In agreement with the results of *Echternacht et al.* [1997] along the PICA profile (see dotted line at 20.5°S in Figure 1 and section 5), our model shows a good conductor beneath the Precordillera. The upper boundary of this structure is near 15 km, while the lower one is not as well resolved. A remarkable result is that the volcanic front itself is not connected with a good conductor as has been found on profiles farther south by *Schwarz and Krüger* [1997].

[31] The most prominent anomaly, a laterally extended (>100 km), extremely conductive structure with resistivities as low as 1 Ω m or even lower in certain regions, can be found beneath the Altiplano. Its upper boundary is undulating between ∼10–30 km, while the lower boundary is not resolved (see discussion below). The root mean square (RMS) error for all sites (B and E polarization) is shown in Figure 5 (middle) as well as the data fit at some representative sites (Figure 5, bottom) and as sections of residuals between model response and data of both polarizations in Figure 6. Here the residuum for apparent resistivity, with a static shift correction incorporated, is calculated as $\Delta \log\rho_a = \log\rho_a^{\mathrm{calc}} - \log\rho_a^{\mathrm{obs}}$. The overall RMS misfit of the shifted data is ∼1.9 compared to 3.44 for the unshifted data.

[32] One of the most evident features of the model given in Figure 5 is the apparent depth extent of the Altiplano Conductivity Anomaly (ACA). Of course, our data do not imply a deep root zone as suggested by the model. Therefore sensitivity studies have been applied to address the vertical extension of this structure. In Figure 5, some isolines of sensitivities are shown. They were calculated by summing up columnwise the absolute values of the error-weighted sensitivity matrix. These sums are normalized by cell area and assigned to the respective grid elements. Further, they are divided by their maximum value which is located somewhere directly beneath the surface. So the labels at the isolines refer to the fraction of maximum sensitivity. A general decrease of sensitivity with depth becomes visible, which is more rapid in the ACA and beneath the Longitudinal Valley. The latter can be explained by the nearby ocean, which prevents the resolution at greater depth [see also *Schwalenberg et al.*, 2002].

[33] In a nonperfect 2-D environment like the Altiplano, E polarization data are often more sensitive to the effects of structure north and south of the profile than B polarization data, and the 2-D inversion of the latter alone may yield a better approximation of the true conductivity distribution than a joint inversion of both modes [*Wannamaker et al.*, 1984; *Wannamaker*, 1999]. Although both approaches show the very good conductor below the Altiplano, the B polarization model looks more unrealistic (very sharp boundaries extending to depths of several hundred kilometers) due to the strong influence of the lateral conductivity boundaries. As can be seen in the apparent resistivity and phase data at many sites (e.g., at PAM) in Figure 7 there is no indication of a more insulating substratum even at the longest periods. Other independ-

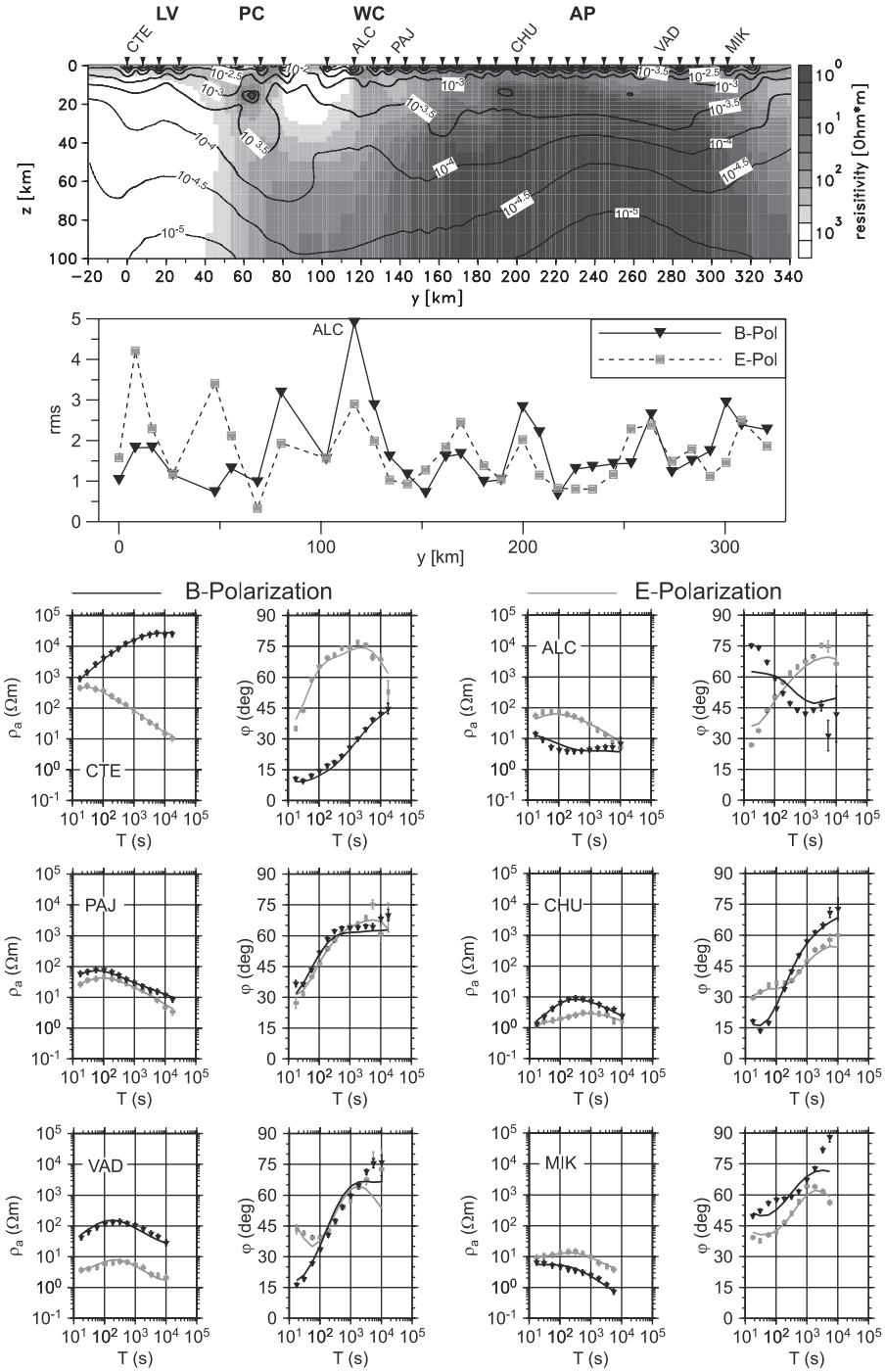

Figure 5. (top) Result of the 2-D inversion. As the calculated resistivities spread over several orders of magnitude, a logarithmic color scale is used. Superimposed are isolines of sensitivities for this model. The sensitivities shown here were calculated by summing up columnwise the error-weighted absolute values of the sensitivity matrix [e.g., *Menke*, 1984]. This sum is normalized by cell area and assigned to the respective grid element [*Schwalenberg*, 2000]. (middle) RMS error for B and E polarization for all sites. The largest misfit occurs at site ALC beneath Olca volcano, where the 2-D assumption is not met (see section 3). (bottom) Model fit at several representative sites. Apparent resistivity data are corrected for static shifts. Strong splitting of the resistivity and phase curves at site CTE is mainly due to ocean effect. See color version of this figure at back of this issue.

ent tests were carried out employing a program by *Siripunvaraporn and Egbert* [2000] which, unlike the code of *Mackie et al.* [1997] that we used, also allows for the inversion of B_z data, in our case the T_{zy} component. Again a good and deep reaching conductor below the Altiplano was resolved with comparable depths and conductivity values; the code of *Mackie et al.* [1997] yielded a better fit, however, and was preferred in this analysis.

[34] To constrain the depth extent, we proceeded as proposed by *Nolasco et al.* [1998]. We systematically changed conductivity of

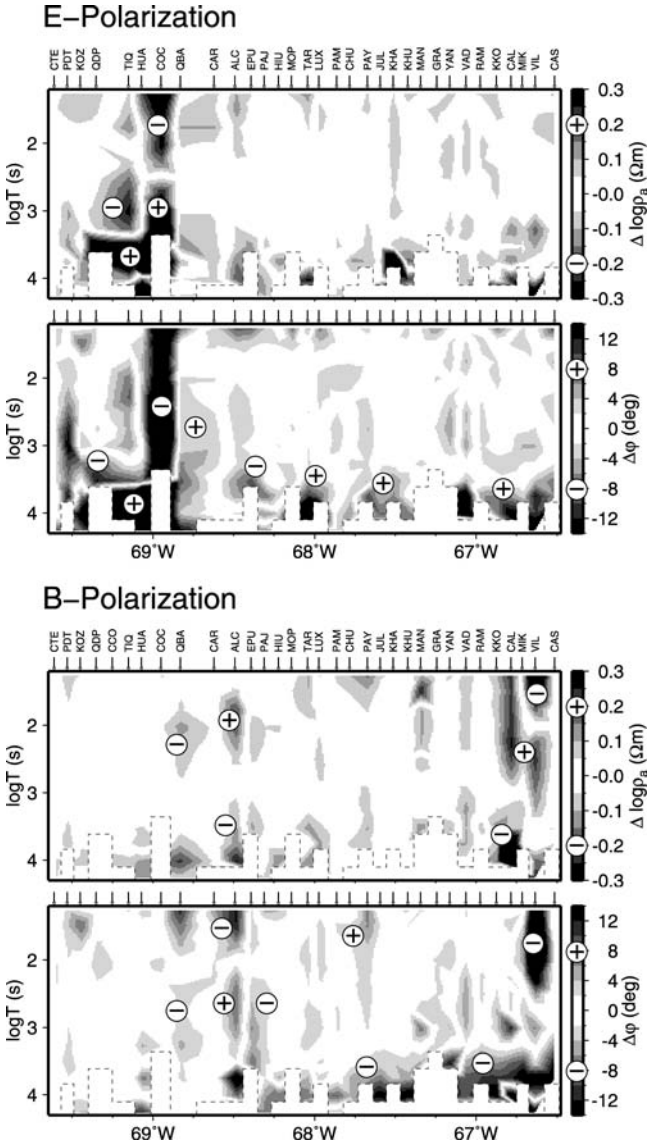

Figure 6. Pseudosections of residuals between response of model given in Figure 5 and data for (top) E and (bottom) B polarization. Observed resistivities were corrected by calculated static shift factors. High deviations at site COC are due to bad data quality; at VIL a strong 3-D effect is observed at short periods. These data were downweighted in the inversion.

selected structures and compared the corresponding model forward responses, keeping in mind that this procedure neglects the interdependence of parameters. In particular, a lower boundary was introduced and lifted up and fixed at 40 or 70 km, respectively (see Figure 7). The model responses of the representative site PAM show that the data fit becomes worse in the E polarization phases for the bottom model while it is in the range of the error bars for the middle one.

[35] Being aware that this kind of sensitivity study does not take into account the dependency between model parameters, it can be ruled out that the ACA ends at depths much less than 50 km which coincides with the 10^{-4} isoline of the sensitivities. Otherwise, more extreme conductivities must be considered to achieve a similar conductance. As a result of these and other sensitivity studies, carried out by *Schwalenberg* [2000] and *Schwalenberg et al.* [2002] and not explicitly mentioned here, a minimum depth extent of the Altiplano conductor of ~60 km with a conductance of more than 20,000 S can be derived.

5. Discussion

[36] In the following, we will discuss the possible causes of the anomalous conductors in this region, concentrating on the Altiplano anomaly. The key to understanding the impressive conductivity anomaly below the Altiplano derives from the comparison with the results from other geophysical methods.

[37] Figure 8 shows a superposition of our final model and a seismic line drawing from the reprocessed ANCORP seismic reflection line [*ANCORP Working Group*, 1999; M. Stiller, personal communication, 1999] as well as the so-called Andean Low-Velocity Zone (ALVZ) derived from receiver function analysis [*Yuan et al.*, 2000], which will be discussed later in this section. Clearly visible is the good agreement beneath the Altiplano, where strong reflections correspond spatially with the upper boundary zone of the Altiplano Conductivity Anomaly (ACA). However, there is no correlation of the downgoing slab (NAZCA reflector) nor the Quebrada Blanca Bright Spot (QBBS) with a conducting zone in our model.

[38] It was suggested that the QBBS results from the entrapment of fluids ascending through the crust. Saline fluids in quantities sufficient to explain the high reflectivity should lead to a significant increase in electrical conductivity. Therefore it would be a strong argument in favor of this explanation, if at least the existence of this structure could be corroborated by electromagnetic methods. However, none of our regularized inversions resulted in a structure which could be correlated to the zone of seismic brightness. In addition, the raw data do not suggest a conductive feature in the area under consideration.

[39] However, we have to consider that the inversion procedure is of the minimum-structure type. Therefore we have to exclude the possibility of missing features as a result of the particular regularization used. To deal with this class of problems, we modified the model in Figure 7 by a conductive zone associated with the bright spot and used the resulting model as a priori information in the inversion process. As emphasized above, the algorithm is then forced to find a model that is close to the a priori model in the chosen seminorm. The data misfit of the inversion result obtained by this procedure is thereby comparable to the data misfit of the ANCORP model in Figure 7. Although, as a result of the kind of regularization we used, a weak zone of increased conductivities remains, it is compensated by a surrounding area of increased resistivity. Thus the inversion attempts to destroy the "disturbing" conductor. Subsequently, we think this structure is not only unnecessary to explain the MT data but even contradicts them [see also *Schwalenberg et al.*, 2002].

[40] It has to be mentioned that the petrophysical interpretation of the structure as fluid-filled fractures is not the only one possible, and it cannot be ruled out from the seismic data that the bright spot itself is an off-line effect, i.e., may represent reflections from structures north and south of the seismic line.

[41] In case of the NAZCA reflector, there is no sign of a downgoing slab in the inversion results in Figure 8, as was reported for other subduction zones, e.g., at the North American West Coast [*Kurtz et al.*, 1986; *Wannamaker et al.*, 1989a, 1989b]. Potentially high conductivity zones directly associated with the slab might be resolvable at different depths. At shallower levels the, probably fractured, oceanic crust could be wet until depths where all the water is released due to pressure of the overlying continental crust; this would coincide with the onset of the seismogenic zone below the Coastal Cordillera. If existent, water-rich sediments should further enhance the conductivities. A second potential zone lies at ~80–100 km depth, where fluids are released in the blueschist-eclogite transition zone. However, none of these potential conductors is visible in our data.

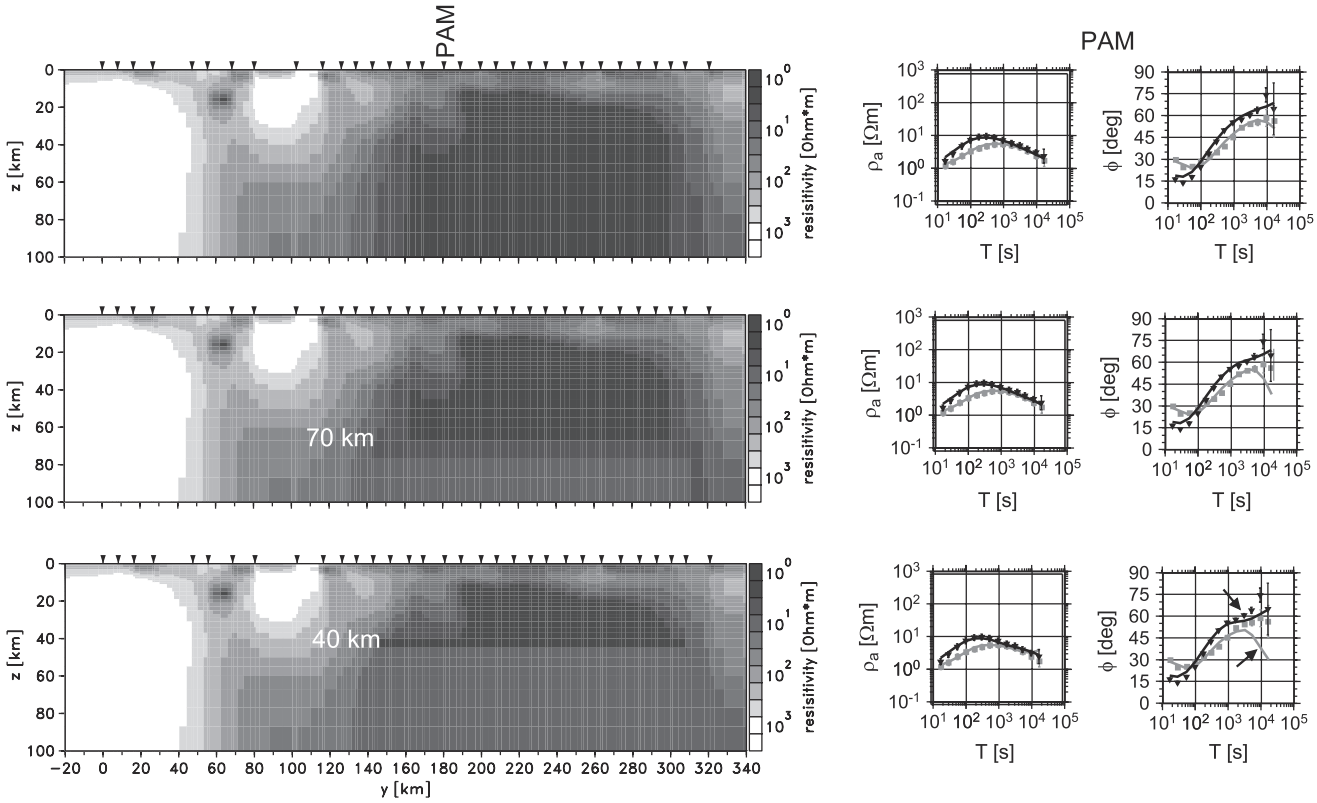

Figure 7. Investigating the depth extent of the Altiplano conductor. (left) Depth to the lower boundary of the highly conductive structure (i.e., $\rho \approx 1\ \Omega$ m), systematically reduced in numerical forward modeling. (right) At a representative site (PAM), with the effect of the lower boundary visible only in the phases at very long periods. Assuming a depth of 70 km, the E polarization phases are just beyond the range of error bars, while a value of 40 km considerably changes phases of both modes at periods $T > 1000$ s (arrows). The other sites show comparable or even smaller effects. See color version of this figure at back of this issue.

[42] A possible explanation for the missing correlation between MT and seismic reflection results is that the data set used in our inversions does not include the areas where the slab is rather shallow and the probability of a large water content is high. The extreme channeling mentioned above at the sites near the coast impedes their further interpretation, and we therefore excluded them from 2-D modeling. This results in low sensitivity values in this area below the Coastal Cordillera and the Longitudinal Valley (see Figure 5), implying that the data used contain nearly no information on this hypothetical structure. Also, the overwhelming lateral influence of the conductivity anomalies of the Pacific Ocean in the west and the ACA in the east reduces detectability. Furthermore, model calculations from *Evans et al.* [2002] imply the necessity of off-shore measurements to resolve the slab as a good conductor.

[43] In analogy to the procedure that we applied with respect to the QBBS (see above) we checked the hypothesis of a conductive slab by adding it as an a priori structure to our final model. The downgoing plate was incorporated as a rather thick zone of lower resistivities (~10 km of 10 Ω m, implying an integrated conductivity of ~1000 S), roughly arranged to coincide with the NAZCA reflector identified by reflection seismology (see Figure 8). Again, both the original model and the biased inversion result gave a comparable misfit. The conductive feature did not "survive" this test in the westernmost highly resistive area, and only a local structure at greater depths remained below the western Precordillera. We conclude that our data do not support this kind of electrical structure, which would coincide with the dehydration processes in and on top of the slab, located below the Longitudinal valley and the Precordillera, although it cannot be totally ruled out. It also remains questionable whether the downgoing slab should be associated with anomalous conductivities, as most of the original fluid content leaves the plate very early, and the fate of the metamorphic water released at depth is far from clear [*Peacock*, 1996, 1990]. As mentioned in section 1, the trench is free of sediments, which may additionally explain the missing conductor.

[44] For comparison, and without going into further detail, a new 2-D inversion result of the PICA profile (Figure 1) is also displayed in Figure 8. The Chilean section of this data set was originally interpreted by *Echternacht* [1998] by 2-D forward modeling; it was later extended by three sites in Bolivia. Here the derived regional strike was −8°. The profile was interpreted up to the Pacific Coast; the ocean itself was kept fixed during the inversion with a resistivity of 0.3 Ω m. Similar features are visible here, e.g., the missing good conductor associated with the downgoing slab and the Precordillera anomaly. The volcanic arc is resistive as at 21°S, and a deep conductor appears beneath the Altiplano, too, although this structure is east of the last site and therefore not well resolved.

[45] Unlike in areas farther south at 22°S, where a good conductor is connected to the volcanic arc, this electrical structure vanishes toward the north. While at least the very eastern part of the Western Cordillera displays high conductivities at 21°S, this feature is completely absent at 20°S along the PICA profile. This is in striking correlation with the gradual disappearance of the zone of seismic attenuation, which is manifested by Q_p quality factors below 100 south of 22°S and more than 500–1000 in the north [*Haberland and Rietbrock*,

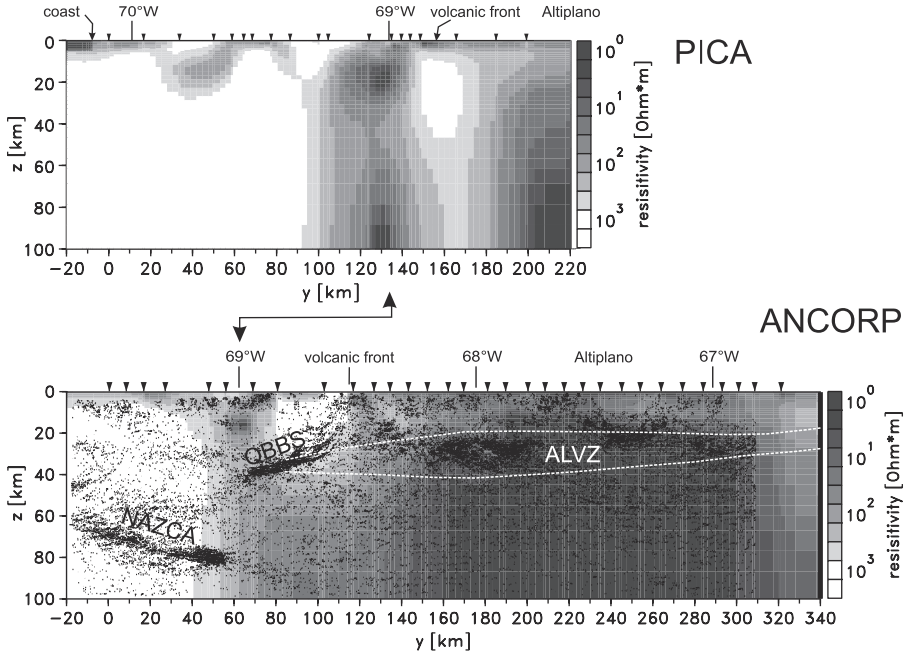

Figure 8. Reflection seismic results (line drawings, redrawn from Stiller (personal communication, 1999)) and the location of the ALVZ (from Andean Low-Velocity Zone) derived from receiver function analysis [*Yuan et al.*, 2000] are superimposed on the MT model. QBBS (Quebrada Blanca Bright Spot) marks the highly reflective zone in the middle crust of the forearc. Also shown is a new 2-D inversion result from the PICA profile, which, for the Chilean side, see Figure 1, was already analyzed by *Echternacht* [1998] using a 2-D forward modeling approach. The ocean has been used as a priori information for both profiles, it is more than 40 km to the west of the westernmost site on the ANCORP profile. See color version of this figure at back of this issue.

2001; *Graeber and Asch*, 1999; *Schmitz et al.*, 1999]. In this region of the Pica Gap, volcanism is pre-Holocene with only one exception, the comparatively small center of Porquesa volcano [*Wörner et al.*, 1994]. Although not well covered by measuring sites, *Haberland and Rietbrock* [2001] found low Q_p values below the ANCORP profile in the western Altiplano. Farther to the north, *Baumont et al.* [1999] also did not find a highly attenuating zone below the Western Cordillera, but they mapped very low Q_p values below the Altiplano with the BANJO and SEDA seismological networks. *Swenson et al.* [2000] deduce a felsic composition of the entire middle and lower Altiplano crust from this data set. It must be kept in mind, however, that these networks were positioned farther to the north of the ANCORP profile and correlations are questionable.

[46] Recent calculations [*Rietbrock and ANCORP Research Group*, 1999] show that the southern Altiplano crust is characterized by an enhanced v_p/v_s ratio of ~1.8. A high v_p/v_s ratio below the north central Altiplano was also detected by *Dorbath and Granet* [1999] and *Myers et al.* [1998]. Finally, the Rayleigh wave study of *Vdovin et al.* [1999] characterizes the whole Altiplano as a region of drastically decreased surface wave velocities compared with the rest of the South American continent.

[47] The location of the Altiplano conductor itself coincides with a spectacular seismic low-velocity zone at depths of roughly 15–20 km, detected by analysis of *P* to *S* converted waves (receiver functions) including data from the BANJO and SEDA as well as the ANCORP network. *Chmielowski et al.* [1999] interpret this very thin anomalous layer (thickness ~1 km) as the Altiplano-Puna magma body and infer partial melt rates of more than 15%. *Yuan et al.* [2000] found a similar but deeper reaching low-velocity zone (ALVZ) below the entire Altiplano-Puna Plateau. This ALVZ was obtained from a network which also included the PUNA data set and is referred to a cross section farther to the south. Nevertheless, there is a good correlation with the upper parts of the high-conductivity zone below the Altiplano (see Figure 8). A low-velocity layer beneath all of the Altiplano was also revealed by reinterpretation of seismic refraction and wide-angle reflection data [*Wigger et al.*, 1994; *Schmitz et al.*, 1997; *Lessel*, 1998]. A recent analysis of wide-angle reflections along the ANCORP profile [*Lüth*, 2000] confirms this result, although the highly attenuating thick sedimentary cover did not permit a clear identification of reflecting boundaries, which display strong lateral variations, throughout the entire Altiplano.

[48] Further geophysical observations exist in this specific part of the central Andes, namely, heat flow measurements and an extensive gravity network. The Altiplano is characterized by high heat flow densities [*Hamza and Muñoz*, 1996; *Henry and Pollack*, 1988]. Figure 9 shows the observed heat flow values in a cross section from the trench to the Chaco, the eastern foreland of the Andes [*Springer and Förster*, 1998; *Springer*, 1999]. Although the database is insufficient in many regions, Figure 9 displays a general trend: heat flow density values increase from 20 mW m^{-2} in the forearc to more than 100 mW m^{-2} in the arc and back arc of the central Andes. *Springer* [1999] calculated a temperature distribution from these data; below the Altiplano the temperature exceeds 600°C at depths of more than 40 km. As can be seen from Figure 9, however, the high heat flow on the Altiplano is not sufficiently explained by this model and the temperature gradient must be greater or other sources (advective heat transport by fluids or melts) have to be taken into account. Altogether, these temperatures would enable partial melting in a wet, predominantly felsic deep crust.

[49] The Altiplano conductivity anomaly is also correlated with a positive isostatic residual gravity anomaly with values of ~30 × 10^{-5} m s^{-2} = 30 mGal (Figure 9) [see *Götze and MIGRA Group*, 1996; *Kirchner et al.*, 1996; *Kirchner*, 1997]. Taking into account

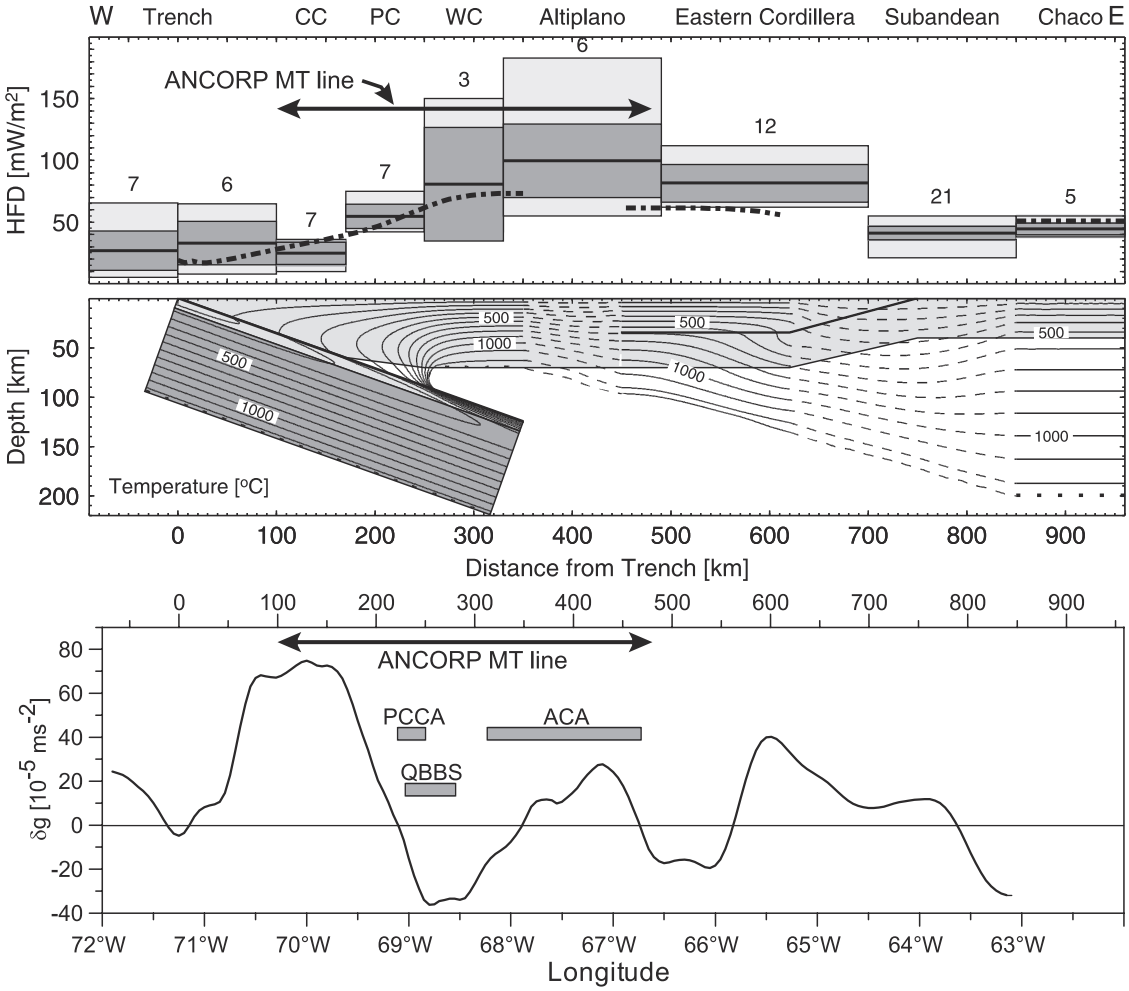

Figure 9. (top) Heat flow density (HFD) and 2-D temperature model of *Springer* [1999] for the central Andes. Confidence limits of HFD values are shaded. The Altiplano itself was not modeled here; accordingly, temperature isolines are dashed. HFD model response is shown as dotted line. (bottom) Isostatic residual field along 21°S, extracted from *Götze and MIGRA Group* [1996]. Gravity values in 10^{-5} m s^{-2} = mGal. The locations of the Altiplano conductivity anomaly (ACA), the Quebrada Blanca Bright Spot (QBBS) and the Precordillera conductivity anomaly (PCCA) are also shown.

its long wavelength, this would infer an extended body of increased density and thus a more mafic composition of the middle and deep crust. There is experimental evidence, however, that partial melting may also enhance the density of wet granitic and intermediate rocks [*Clemens and Droop*, 1998].

[50] There exist basically two explanations for the high conductivities: saline brines and partial melts. Other theoretically possible candidates may be excluded: Neither highly connected graphite at grain boundaries nor extensive ore bodies are in accordance with the low-velocity zone. Although graphite precipitated along shear planes has been found responsible for many zones of enhanced conductivity in the middle crust throughout the world [e.g., *ELEKTB Group*, 1997], an interconnected network is unlikely to be stable in an active orogen [*Katsube and Mareschal*, 1993; *Wannamaker*, 2000].

[51] The key to discriminate between fluids and partial melts lies in the temperature regime, and unfortunately, this is the least constrained of all physical parameters derived in the Andes. The relatively low gradient according to the model calculations of *Springer* [1999] would raise the temperatures above the solidus of granitic or even intermediate rocks at depths below ~40 km. Recent estimates of F. R. Schilling (personal communication, 2000) taking into account the temperature-pressure dependence of thermal conductivity lead to a much higher gradient in the upper crust, and therefore partial melting would be enabled already at depths of ~20 km.

[52] *Schilling et al.* [1997] and *Schilling and Partzsch* [2001] explained the observed conductivities below the Western Cordillera at 22°–23°S (south of the area studied here) with partial melt rates exceeding 14% by carrying out laboratory measurements and theoretical calculations employing a modified brick layer model (MBL), which gives comparable values as the upper Hashin-Shtrikman bound (HS_+) for a completely interconnected network. *Partzsch et al.* [2000] extended this work and applied the partial melt approach to other regions, namely, the Pyrenees and the Tibetan Plateau, where prominent highly conductive zones, though with smaller conductivities and conductances as in the Andes, have been found [*Pous et al.*, 1995; *Nelson et al.*, 1996]. *Schilling et al.* [1997] assumed a solid rock conductivity of σ_{rock} = 0.005 S m^{-1} with the melt conductivity set to σ_{melt} = 10 S m^{-1}. If σ_{rock} is set to 0.001 S m^{-1}, a HS_+ bulk conductivity of 1 S m^{-1} would be achieved with melt rates of 10%, whereby a value of 10 S m^{-1} has to be regarded as an upper limit for the conductivity of granitic melt. Since laboratory data are usually obtained on dry samples, the melting temperatures are usually much higher (>1000°C) than probably occur in the wet, granitic deeper crust of the Altiplano,

and there exist no laboratory data which were achieved under these conditions.

[53] All other observed anomalies suggest this explanation with the possible exception of the positive residual gravity anomaly: high v_p/v_s ratios, low Q_p quality factors, low seismic velocities, and a high heat flow density. For the location of the BANJO/SEDA networks north of 20°S, *Swenson et al.* [2000] and *Baumont et al.* [1999] do not consider the assumption of partial melts and attribute their low Q_p values purely to scattering and the low seismic velocities to an overall felsic composition of the crust, deriving a "normal" Poisson ratio of 0.25 from their observed v_p/v_s values. As mentioned above, there are no electromagnetic data available in the central Altiplano north of 21°S (there are hints from the easternmost sites on the PICA profile, however, suggesting a low-resistivity zone at 20°S below the Altiplano), which could indicate a fluid/partial melt content and thus discriminate between these possibilities; the "Andean Conductor" detected by *Schmucker et al.* [1966] is located even farther north. For the region south of the Salar de Uyuni a slightly higher Poisson number (0.27–0.28) can be derived, still not enough to account for substantial amounts of melt. However, interconnected melts at grain edges, not along the surfaces, could explain this observation. This would place an upper bound of ~10% on the possible melt proportion, still in accordance with the high electrical conductivities.

[54] Of course, we cannot rule out the presence of saline fluids, especially in the upper parts of the Altiplano conductor, which would explain the strong seismic reflectivity in the middle crust, too. It is also difficult to address the problem of the melt origin (i.e., migration from the asthenospheric wedge or in situ melting due to fluid influx and rise of temperature) from the magnetotelluric results as this would require more reliable data at very long periods. The 2-D models suggest a continuation of the high-conductivity zone toward great depths below the western Altiplano and the Altiplano-Puna Volcanic Zone and thus a connection with the asthenospheric wedge. However, from the sensitivity studies presented earlier, a clear resolution of this feature from the existing data set seems impossible.

[55] No matter whether the conductivity anomaly is attributed purely to melts or brines or a combination of both (possibly at different depths), the middle and lower Altiplano crust has to be regarded as a zone of rheological weakness. There is geological evidence that no deformation of the upper crust has occurred since the late Tertiary [*Allmendinger and Gubbels*, 1996]. Taking into account the actual movement vectors derived from GPS measurements [*Klotz*, 2000], which show quasi-undisturbed velocities of 2 cm yr^{-1} in WSW direction from the Western Cordillera across the whole southern Altiplano until the Eastern Cordillera, it may be speculated that the upper crust moves as a stable block above the high-conductivity (and low-velocity) zone. Here, at 20°–21°S or even farther to the north, the Western Cordillera is resistive and may not act as a rheological buffer. The situation is completely different in the south, where movement is halted by the Western Cordillera, which is highly conductive and acts as rheological buffer. Consequently, horizontal movement vectors are an order of magnitude smaller in the Puna part of the high plateau.

6. Conclusions

[56] The extraordinary electrical conductivity anomaly in the middle and lower crust beneath the Bolivian Altiplano has been revealed as an effect of first-order by long-period magnetotelluric investigations. It was treated as a two-dimensional structure, and although this is justified by a dimensionality analysis for large parts of the main ANCORP profile, certain areas clearly show more complicated electrical features. This is especially manifested in the behavior of the induction arrows, which were not incorporated into the model-finding process. The sites near the Chilean coast display not only deviations from the expected W-E arrow direction (coast effect) but also strong telluric distortions due to current channeling in an elongated conductor presumably connected to the Atacama Fault System. They were not included in the interpretation and obviously deserve further attention. Another problematic data subset from the Precordillera also shows N-S pointing induction arrows; unfortunately, the inaccessibility of this mountain chain impedes a better sampling of the discovered anomaly in the middle crust. The depth extent of the Altiplano anomaly could not be clearly resolved due to the lack of reliable transfer functions at periods exceeding 10,000 s. A quasi-observatory operation of stations would be required to solve this important question.

[57] Another topic worth considering would be the N-S elongation of the Altiplano conductor. Modeling of the more northern PICA profile also showed a conductor at depth below the plateau, but an extension of this data set to the east is clearly necessary. A confirmation of a highly conductive zone beneath the central Altiplano would add to the understanding of other major observed geophysical anomalies, mainly the high attenuation of seismic waves. Altogether the current electromagnetic study reveals the middle and deep crust of the southern Altiplano as a zone of rheological weakness, an observation which should have a distinct impact on the attempts to understand the structure and evolution of the high plateau.

[58] **Acknowledgments.** We have to thank many coworkers for their help in the field, namely J. Beike, S. Friedel (who also processed the Bolivian data), W. Heise, M. Muñoz, P. Salazar, A. Sanchez, and F. Ticona. We gratefully acknowledge the support of L. Baeza, G. Behn (both Codelco Chile), G. Chong Diaz, H. Wilke (Universidad Católica del Norte, Antofagasta), R. Röling, S. Tawackoli (SERGEOMIN, La Paz), and E. Ricaldi (Universidad Mayor de San Andrés, La Paz). Many discussions, especially with P. Giese, E. Scheuber, F. Schilling, and P. Wigger, clarified the geological and petrophysical significance. The very constructive reviews of J. Booker, S. Park, and G. Zandt helped to improve the manuscript. This work was funded by the Deutsche Forschungsgemeinschaft (DFG) within the framework of the Collaborative Research Project SFB 267 Deformation Processes in the Andes. P. Lezaeta was supported by Deutscher Akademischer Austauschdienst (DAAD). We would like to honor our friend and colleague Gerardo Behn, who passed away in Santiago de Chile in July 2001.

References

Allmendinger, R. W., and T. Gubbels, Pure and simple shear plateau uplift, Altiplano-Puna, Argentina and Bolivia, *Tectonophysics*, *259*, 1–13, 1996.

Allmendinger, R. W., T. E. Jordan, S. M. Kay, and B. L. Isacks, The evolution of the Altiplano-Puna Plateau of the central Andes, *Annu. Rev. Earth Planet. Sci.*, *25*, 139–174, 1997.

ANCORP Working Group, Seismic reflection image revealing offset of Andean subduction-zone earthquake locations into oceanic mantle, *Nature*, *397*, 341–344, 1999.

Bahr, K., Interpretation of the magnetotelluric impedance tensor: Regional induction and local telluric distortion, *J. Geophys.*, *62*, 119–127, 1988.

Bahr, K., Geological noise in magnetotelluric data: a classification of distortion types, *Phys. Earth Planet. Inter.*, *66*, 24–38, 1991.

Baumont, D., A. Paul, S. L. Beck, and G. Zandt, Strong crustal heterogeneity in the Bolivian Altiplano as suggested by attenuation of *Lg* waves, *J. Geophys. Res.*, *104*, 20,287–20,305, 1999.

Beck, S. L., G. Zandt, S. C. Myers, T. C. Wallace, P. G. Silver, and L. Drake, Crustal thickness variations in the central Andes, *Geology*, *24*, 407–410, 1996.

Beck, S. L., J. Swensson, and G. Zandt, The cause of thick, slow crust in the Altiplano, central Andes: Melt or composition?, paper presented at 4th International Symposium on Andean Geodynamics, Orstom, Göttingen, Germany, 1999.

Beike, J., Studien zur anisotropen Leitfähigkeitsverteilung und ein Versuch zur Erklärung magnetotellurischer Übertragungsfunktionen in der Küstenkordillere Nordchiles, Diplomarbeit, Inst. für Geol. Wiss., Freie Univ. Berlin, Berlin, 2001.

Chave, A. D., and J. T. Smith, On electric and magnetic galvanic distortion tensor decompositions, *J. Geophys. Res.*, *99*, 4669–4682, 1994.

Chmielowski, J., G. Zandt, and C. Haberland, The central Andean Altiplano-Puna magma body, *Geophys. Res. Lett.*, *26*, 783–786, 1999.

Clemens, J. D., and G. T. R. Droop, Fluids, P-T paths and the fates of anatectic melts in the Earth's crust, *Lithos*, *44*, 21–36, 1998.

de Silva, S. L., Altiplano-Puna volcanic complex of the central Andes, *Geology*, *17*, 1102–1106, 1989.

de Silva, S. L., and P. W. Francis, *Volcanoes of the Central Andes*, Springer-Verlag, New York, 1991.

Dorbath, C., and M. Granet, Local earthquake tomography of the Altiplano and the Eastern Cordillera of northern Bolivia, *Tectonophysics*, *259*, 117–136, 1999.

Echternacht, F., Die elektrische Leitfähigkeitsstruktur im Forearc der südlichen Zentralanden bei 20°–21°S, abgeleitet aus magnetotellurischen und geomagnetischen Sondierungen, *Sci. Tech. Rep. 98/20*, GFZ Potsdam, Germany, 1998.

Echternacht, F., S. Tauber, M. Eisel, H. Brasse, G. Schwarz, and V. Haak, Electromagnetic study of the active continental margin in northern Chile, *Phys. Earth Planet. Inter.*, *102*, 69–87, 1997.

Egbert, G. D., and J. R. Booker, Robust estimation of geomagnetic transfer functions, *Geophys. J. R. Astron. Soc.*, *87*, 173–194, 1986.

ELEKTB Group, KTB and the electrical conductivity of the crust, *J. Geophys. Res.*, *102*, 18,289–18,306, 1997.

Evans, R. L., A. D. Chave, and J. R. Booker, On the importance of offshore data for magnetotelluric studies of ocean-continent subduction systems, *Geophys. Res. Lett.*, *29*, 10.1029/2001GL013960, in press, 2002.

Gamble, T., W. Goubau, and J. Clarke, Magnetotellurics with a remote reference, *Geophysics*, *44*, 53–68, 1979.

Giese, P., E. Scheuber, F. R. Schilling, M. Schmitz, and P. J. Wigger, Crustal thickening processes in the central Andes and the different natures of the Moho-discontinuity, *J. S. Am. Earth Sci.*, *12*, 201–220, 1999.

Götze, H.-J., and MIGRA Group, Group updates the gravity data base in the Central Andes (20°–26°S), *Eos Trans. AGU Electron. Suppl.*, 1996. (Available as http://www.agu.org/eos_elec/95189e.html.)

Götze, H.-J., B. Lahmeyer, S. Schmidt, and S. Strunk, The lithospheric structure of the central Andes (20°–26°S) as inferred from interpretation of regional gravity, in *Tectonics of the Southern Central Andes*, edited by K.-J. Reutter, E. Scheuber, and P. J. Wigger, pp. 7–21, Springer-Verlag, New York, 1994.

Graeber, F., and G. Asch, Three dimensional models of p-wave velocity and p-to-s velocity ratio in the southern central Andes by simultaneous inversion of local earthquake data, *J. Geophys. Res.*, *104*, 20,237–20,256, 1999.

Groom, R. W., and R. C. Bailey, Decomposition of magnetotelluric impedance tensors in presence of local three-dimensional galvanic distortion, *J. Geophys. Res.*, *94*, 1913–1925, 1989.

Haberland, C., and A. Rietbrock, Attenuation tomography in the western central Andes: A detailed insight into the structure of a magmatic arc, *J. Geophys. Res.*, *106*, 11,151–11,167, 2001.

Hamza, V. M., and M. Muñoz, Heat flow map of South America, *Geothermics*, *25*, 599–646, 1996.

Henry, S., and H. Pollack, Terrestrial heat flow above the Andean subduction zone in Bolivia and Peru, *J. Geophys. Res.*, *93*, 15,153–15,162, 1988.

Isacks, B. L., Uplift of the central Andean plateau and bending of the Bolivian Orocline, *J. Geophys. Res.*, *93*, 3211–3231, 1988.

James, D. E., Andean crustal and upper mantle structure, *J. Geophys. Res.*, *76*, 3246–3271, 1971.

Janssen, C., A. Hoffmann-Rothe, S. Tauber, and H. Wilke, Internal structure of the Precordilleran fault system (Chile)—Insights from structural and geophysical observations, *J. Struct. Geol.*, *24*, 123–143, 2001.

Katsube, T. J., and M. Mareschal, Petrophysical model of deep electrical conductors: Graphite lining as a source and its disconnection due to uplift, *J. Geophys. Res.*, *98*, 8019–8030, 1993.

Kirchner, A., 3D-Dichtemodellierung zur Anpassung des Schwere- und des Schwerepotentialfeldes der zentralen Anden, *Berl. Geowiss. Abh., Ser. B, 25*, 1997.

Kirchner, A., H.-J. Götze, and M. Schmitz, 3D-Density Modelling with Seismic Constraints in the central Andes, *Phys. Chem. Earth*, *21*, 289–293, 1996.

Klotz, J., Geodätische Untersuchungen zur Deformation aktiver Kontinentalränder, Habilitationsschrift, Fachbereich Geowissenschaften, Tech. Univ. Berlin, Berlin, 2000.

Kurtz, R. D., J. M. Delaurier, and J. C. Gupta, A magnetotelluric sounding across Vancouver Island detects the subducting Juan de Fuca plate, *Nature*, *321*, 596–599, 1986.

Lamb, S., and L. Hoke, Origin of the high plateau in the central Andes, Bolivia, South America, *Tectonics*, *16*, 623–649, 1997.

Lessel, K., Die Krustenstruktur der Zentralen Anden in Nordchile (21–24°S), abgeleitet aus 3D-Modellierungen refraktionsseismischer Daten, *Berl. Geowiss. Abh., Ser. B*, *31*, 1998.

Lezaeta, P., Distortion analysis and 3-D modeling of magnetotelluric data in the southern central Andes, Ph.D. thesis, Fachber. Geowiss., Freie Univ. Berlin, Berlin, 2001.

Lezaeta, P., M. Muñoz, and H. Brasse, Magnetotelluric image of the crust and upper mantle in the backarc of the NW Argentinean Andes, *Geophys. J. Int.*, *142*, 841–854, 2000.

Lüth, S., Ergebnisse weitwinkelseismischer Untersuchungen und die Struktur der Kruste auf einer Traverse über die Anden bei 21°S, Ph.D. thesis, Fachber. Geowiss., Freie Univ. Berlin, Berlin, 2000.

Mackie, R., S. Rieven, and W. Rodi, Users manual and software documentation for two-dimensional inversion of magnetotelluric data, GSY-USA, Inc., San Francisco, Calif., 1997.

Menke, W., *Geophysical Data Analysis: Discrete Inverse Theory*, Academic, San Diego, Calif., 1984.

Myers, S. C., S. Beck, G. Zandt, and T. Wallace, Lithospheric-scale structure across the Bolivian Andes from tomographic images of velocity and attenuation for *P* and *S* waves, *J. Geophys. Res.*, *103*, 21,233–21,252, 1998.

Nelson, K., et al., Partially molten middle crust beneath southern Tibet: An initial synthesis of Project INDEPTH results, *Science*, *274*, 1684–1688, 1996.

Nolasco, R., P. Tarits, J. Filloux, and A. Chave, Magnetotelluric imaging of the society islands hotspot, *J. Geophys. Res.*, *103*, 287–309, 1998.

Okaya, N., S. Tawackoly, and P. Giese, Area-balanced model of the late Cenozoic tectonic evolution of the central Andean arc and back arc (lat. 20°–22°S), *Geology*, *25*, 367–370, 1997.

Partzsch, G., F. Schilling, and J. Arndt, The influence of partial melting on the electrical behavior of crustal rocks: Laboratory examinations, model calculations and geological interpretations, *Tectonophysics*, *317*, 189–203, 2000.

Peacock, S. M., Numerical simulation of metamorphic pressure-temperature-time paths and fluid production in subducting slabs, *Tectonics*, *9*, 1197–1211, 1990.

Peacock, S. M., Thermal and petrologic structure of subduction zones, in *Subduction: Top to Bottom*, *Geophys. Monogr. Ser.*, vol. 96, edited by G. Bebout et al., pp. 119–133, AGU, Washington, D. C., 1996.

Pous, J., J. Ledo, A. Marcuello, and M. Daignieres, Electrical resistivity model of the crust and upper mantle from a magnetotelluric survey through the central Pyrenees, *Geophys. J. Int.*, *121*, 750–762, 1995.

Rietbrock, A., and ANCORP Research Group, Velocity structure and seismicity in the central Andes of northern Chile and southern Bolivia, Eos Trans. AGU, *80*(46), Fall Meet. Suppl., F1059, 1999.

Rodi, W., and R. L. Mackie, Nonlinear conjugate gradients algorithm for 2-D magnetotelluric inversions, *Geophysics*, *66*, 174–187, 2001.

Scheuber, E., *Tektonische Entwicklung des nordchilenischen aktiven Kontinentalrandes: Der Einfluß von Plattenkonvergenz und Rheologie, Geotekt. Forsch.*, vol. 81, Schweizerbart, Stuttgart, Germany, 1994.

Schilling, F., and G. Partzsch, Quantifying Partial Melt Fraction in the Crust beneath the central Andes and the Tibetan Plateau, *Phys. Chem. Earth*, *26*, 239–246, 2001.

Schilling, F. R., G. M. Partzsch, H. Brasse, and G. Schwarz, Partial melting below the magmatic arc in the central andes deduced from geoelectromagnetic field experiments and laboratory data, *Phys. Earth Planet. Inter.*, *103*, 17–32, 1997.

Schmitz, M., A balanced model of the southern central Andes, *Tectonics*, *13*, 484–492, 1994.

Schmitz, M., W.-D. Heinsohn, and F. R. Schilling, Seismic, gravity and petrological evidence for partial melt beneath the thickened central Andean crust (21–23°S), *Tectonophysics*, *270*, 313–326, 1997.

Schmitz, M., et al., The crustal structure of the central Andean forearc and magmatic arc as derived from seismic studies—The PISCO 94 experiment in northern Chile (21–23°S), *J. S. Am. Earth Sci.*, *12*, 237–260, 1999.

Schmucker, U., S. E. Forbush, O. Hartmann, A. A. Giesecke, M. Casaverde, J. Castillo, R. Salgueiro, and S. del Pozo, Electrical conductivity anomaly under the Andes, *Year Book Carnegie Inst. Washington*, *65*, 11–28, 1966.

Schwalenberg, K., Die Leitfähigkeitsstruktur der Zentralen Anden bei 21°S: Zweidimensionale Modellstudien und Untersuchungen zur Auflösbarkeit, Ph.D. thesis, Fachber. Geowiss., Freie Univ. Berlin, Berlin, 2000.

Schwalenberg, K., V. Rath, and V. Haak, Sensitivity studies applied to a 2-D resistivity model from the central Andes, *Geophys. J. Int.*, in press, 2002.

Schwarz, G., and D. Krüger, Resistivity cross section through the southern central Andes as inferred from magnetotelluric and geomagnetic deep soundings, *J. Geophys. Res.*, *102*, 11,957–11,978, 1997.

Siripunvaraporn, W., and G. Egbert, An efficient data-subspace inversion for two-dimensional magnetotelluric data, *Geophysics*, *65*, 791–803, 2000.

Springer, M., Interpretation of heat-flow density in the central Andes, *Tectonophysics*, *306*, 377–395, 1999.

Springer, M., and A. Förster, Heatflow density across the central Andean subduction zone, *Tectonophysics*, *291*, 123–139, 1998.

Swenson, J. L., S. L. Beck, and G. Zandt, Crustal structure of the Altiplano from broadband regional waveform modeling: Implications for the composition of thick continental crust, *J. Geophys. Res.*, *105*, 607–621, 2000.

Vdovin, O., J. A. Rial, A. Levshin, and M. Ritzwoller, Group-velocity tomography of South America and the surrounding oceans, *Geophys. J. Int.*, *136*, 324–340, 1999.

von Huene, R., W. Weinrebe, and F. Heeren, Subduction erosion along the North Chile margin, *J. Geodyn.*, *27*, 345–358, 1999.

Wannamaker, P. E., Affordable Magnetotellurics: Interpretation in Natural Environments, in *Three-Dimensional Electromagnetics*, edited by M. Oristaglio and B. Spies, pp. 349–374, Soc. of Explor. Geophys., Tulsa, Okla., 1999.

Wannamaker, P. E., Comments on "The petrologic case for a dry lower crust" by Bruce W. D. Yardley and John W. Valley, *J. Geophys. Res.*, *105*, 6057–6064, 2000.

Wannamaker, P. E., G. W. Hohmann, and S. H. Ward, Magnetotelluric responses of three-dimensional bodies in layered earths using integral equations, *Geophysics*, *49*, 1517–1534, 1984.

Wannamaker, P. E., et al., Magnetotelluric observations across the Juan de Fuca subduction system in the EMSLAB project, *J. Geophys. Res.*, *94*, 14,111–14,125, 1989a.

Wannamaker, P. E., J. R. Booker, A. G. Jones, A. D. Chave, J. H. Filloux, H. S. Waff, and L. K. Law, Resistivity cross-section through the Juan de Fuca subduction system and its tectonic implications, *J. Geophys. Res.*, *94*, 14,127–14,144, 1989b.

Wigger, P. J., et al., Variation in the crustal structure of the southern central Andes deduced from seismic refraction investigations, in *Tectonics of the Southern Central Andes*, edited by K.-J. Reutter, E. Scheuber, and P. J. Wigger, pp. 23–48, Springer-Verlag, New York, 1994.

Wörner, G., S. Moorbath, S. Horn, J. Entenmann, R. S. Harmon, J. P. Davidson, and L. Lopez-Escobar, Large- and fine-scale geochemical variations along the Andean arc of northern Chile (17.5°–22°S), in *Tectonics of the Southern Central Andes*, edited by K.-J. Reutter, E. Scheuber, and P. J. Wigger, pp. 77–92, Springer-Verlag, New York, 1994.

Yuan, X., et al., Subduction and collision processes in the central Andes constrained by converted seismic phases, *Nature*, *408*, 958–961, 2000.

H. Brasse and W. Soyer, Fachrichtung Geophysik, FU Berlin, Malteserstr. 74-100, D-12249 Berlin, Germany. (h.brasse@geophysik.fu-berlin.de; w.soyer@geophysik.fu-berlin.de)

V. Haak, GeoForschungsZentrum Potsdam, Telegrafenberg, D-14473 Potsdam, Germany. (vhaak@gfz-potsdam.de)

P. Lezaeta, Woods Hole Oceanographic Institution, MS 9, Woods Hole, MA 02543-10503, USA. (plezaeta@whoi.edu)

V. Rath, Angewandte Geophysik, RWTH Aachen, Lochnerstr 4-20, D-52056 Aachen, Germany. (v.rath@geophysik.rwth-aachen.de)

K. Schwalenberg, Department of Physics, University of Toronto, 60 St George Street, Toronto, Ontario, Canada M5S 1A7. (katrin@physics.utoronto.ca)

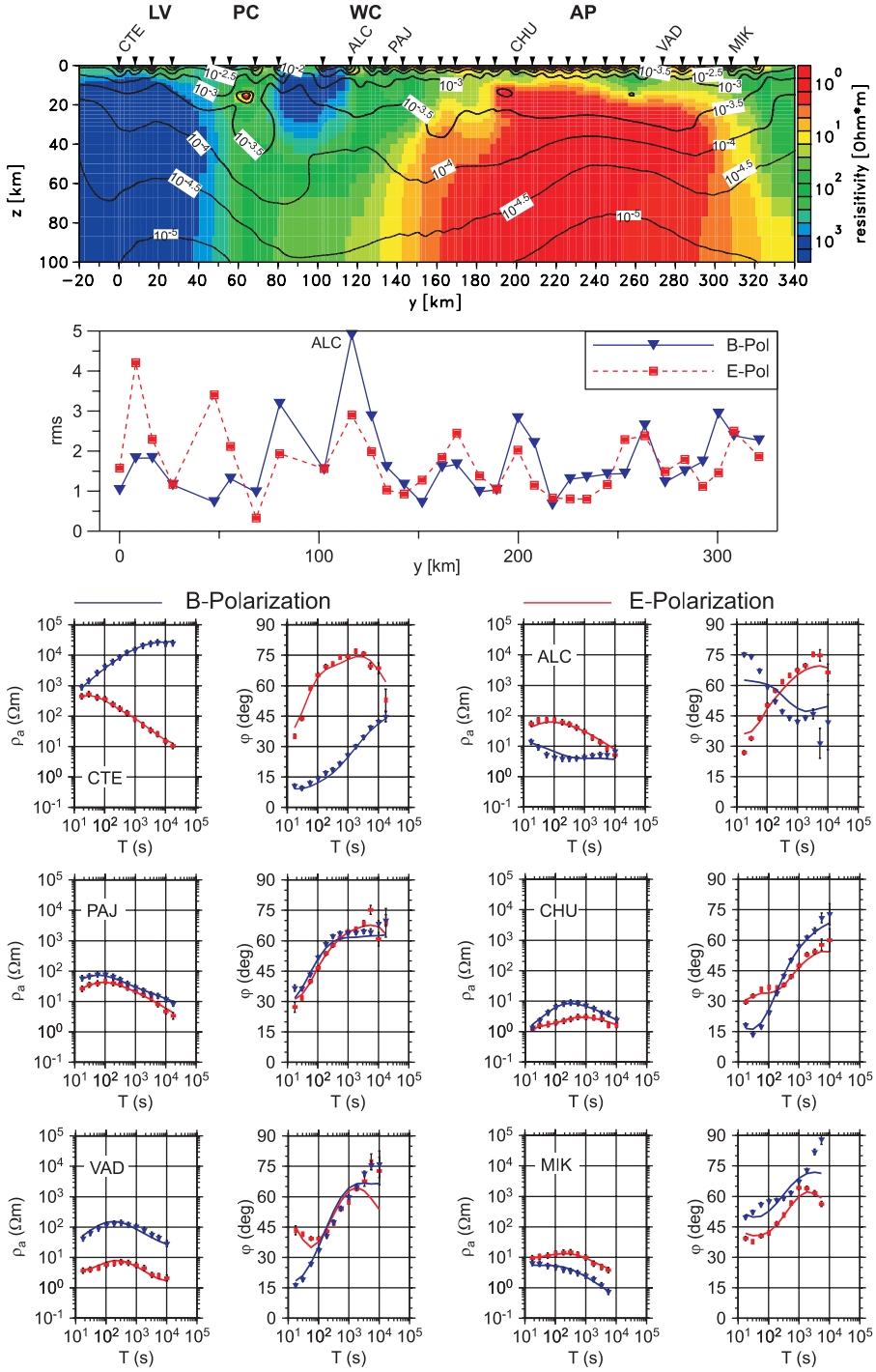

Figure 5. (top) Result of the 2-D inversion. As the calculated resistivities spread over several orders of magnitude, a logarithmic color scale is used. Superimposed are isolines of sensitivities for this model. The sensitivities shown here were calculated by summing up columnwise the error-weighted absolute values of the sensitivity matrix [e.g., *Menke*, 1984]. This sum is normalized by cell area and assigned to the respective grid element [*Schwalenberg*, 2000]. (middle) RMS error for B and E polarization for all sites. The largest misfit occurs at site ALC beneath Olca volcano, where the 2-D assumption is not met (see section 3). (bottom) Model fit at several representative sites. Apparent resistivity data are corrected for static shifts. Strong splitting of the resistivity and phase curves at site CTE is mainly due to ocean effect.

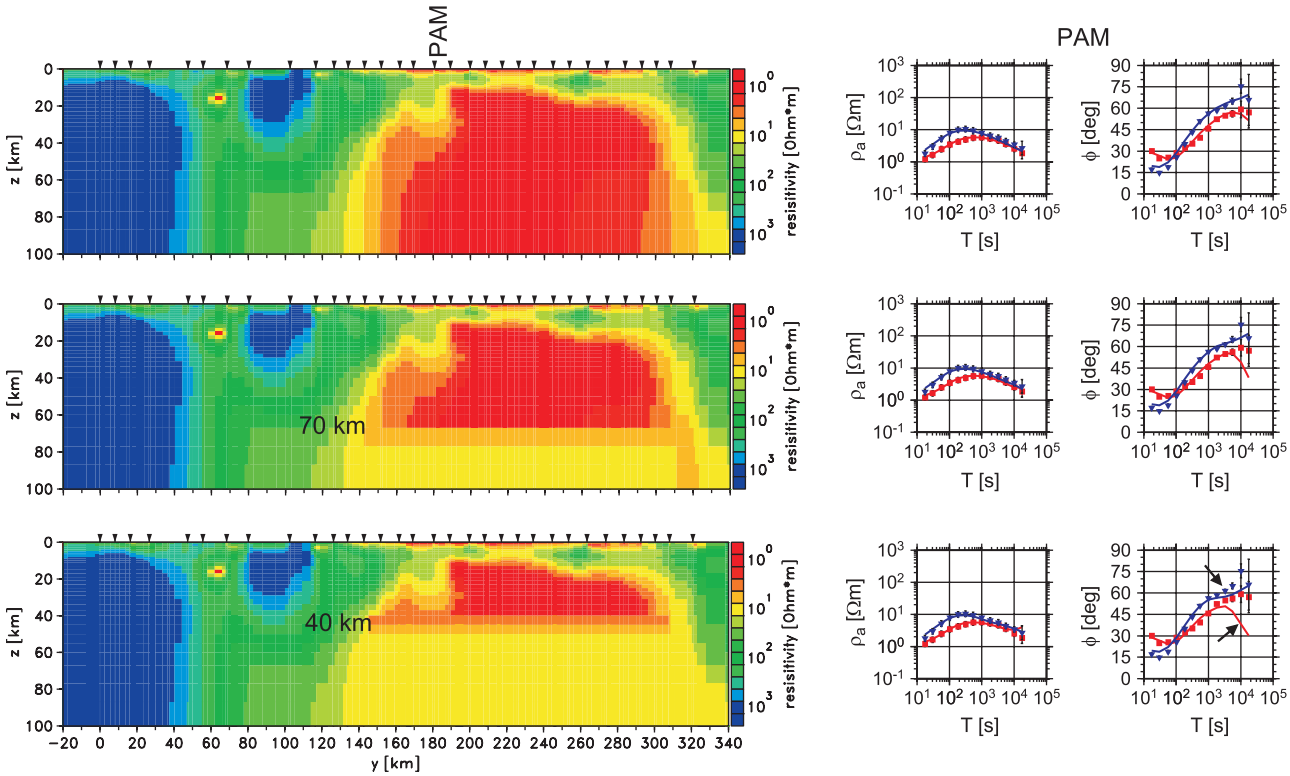

Figure 7. Investigating the depth extent of the Altiplano conductor. (left) Depth to the lower boundary of the highly conductive structure (i.e., $\rho \approx 1\ \Omega$ m), systematically reduced in numerical forward modeling. (right) At a representative site (PAM), with the effect of the lower boundary visible only in the phases at very long periods. Assuming a depth of 70 km, the E polarization phases are just beyond the range of error bars, while a value of 40 km considerably changes phases of both modes at periods $T > 1000$ s (arrows). The other sites show comparable or even smaller effects.

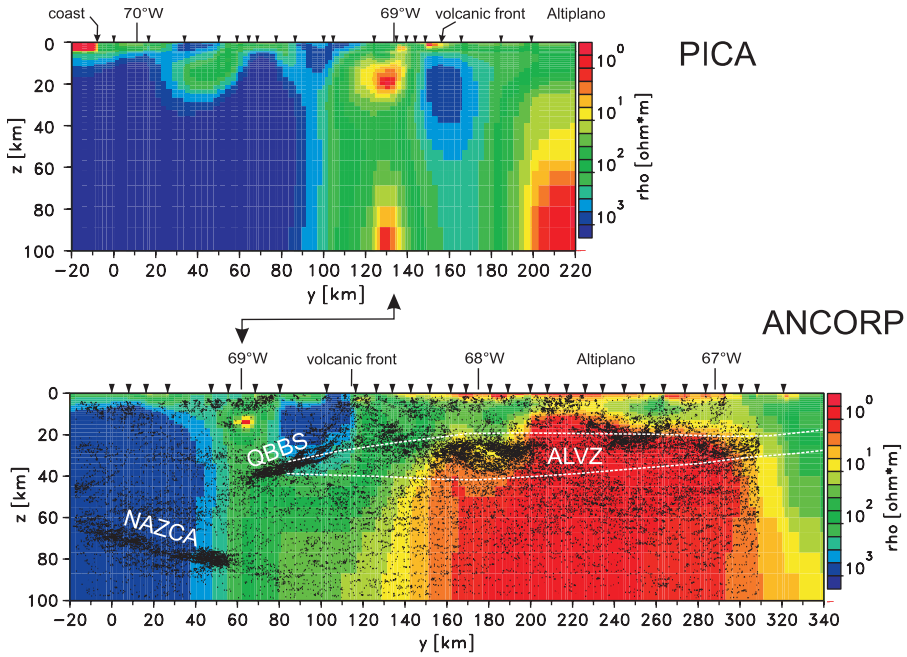

Figure 8. Reflection seismic results (line drawings, redrawn from Stiller (personal communication, 1999)) and the location of the ALVZ (from Andean Low-Velocity Zone) derived from receiver function analysis [*Yuan et al.*, 2000] are superimposed on the MT model. QBBS (Quebrada Blanca Bright Spot) marks the highly reflective zone in the middle crust of the forearc. Also shown is a new 2-D inversion result from the PICA profile, which, for the Chilean side, see Figure 1, was already analyzed by *Echternacht* [1998] using a 2-D forward modeling approach. The ocean has been used as a priori information for both profiles, it is more than 40 km to the west of the westernmost site on the ANCORP profile.